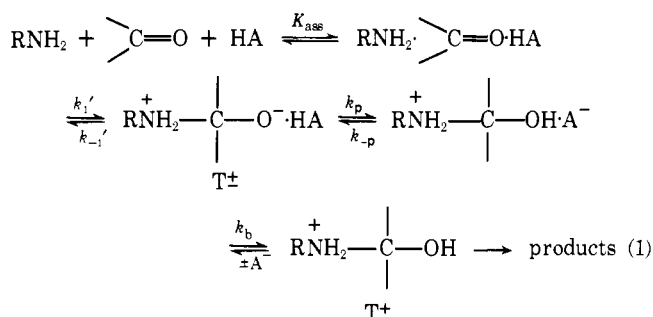bifunctional catalysts are more active by factors of up to 200.

The nonlinear Brønsted plot for monofunctional catalysts is consistent with the preassociation mechanism of eq 1 in

$$RNH_2 + \,>\!\!C\!\!=\!\!O + HA \underset{}{\overset{K_{ass}}{\rightleftharpoons}} RNH_2 \cdot \,>\!\!C\!\!=\!\!O \cdot HA$$

$$\underset{k_{-1}'}{\overset{k_1'}{\rightleftharpoons}} \; RNH_2\!\!-\!\!\overset{+}{\underset{|}{C}}\!\!-\!\!O^-\!\cdot HA \; \underset{k_{-p}}{\overset{k_p}{\rightleftharpoons}} \; RNH_2\!\!-\!\!\overset{+}{\underset{|}{C}}\!\!-\!\!OH\!\cdot A^-$$
$$T^{\pm}$$

$$\underset{\pm A}{\overset{k_b}{\rightleftharpoons}} \; RNH_2\!\!-\!\!\overset{+}{\underset{|}{C}}\!\!-\!\!OH \longrightarrow \text{products} \quad (1)$$
$$T^+$$

which the different regions of the Brønsted plot represent three different rate-determining steps: k_1', k_p, and k_b for strong, weaker, and weak acids, respectively.

The following evidence supports the preassociation mechanism. (1) The curvature cannot be accounted for by a trapping mechanism involving only diffusion and proton-transfer steps. The "Eigen curve" for such a mechanism,[5] based on a calculated pK[6] of 6.5 for T$^+$, is shown as the dotted line in Figure 1; catalysis by a trapping mechanism has been shown to follow Eigen curves for more basic amine nucleophiles.[2] (2) The limiting slope of the Brønsted plot is $\alpha = 0.16$, consistent with catalysis of amine addition by hydrogen bonding,[7] and not with the value of $\alpha = 0$ that is required for diffusion-controlled proton transfer.[5] (3) The proton fits on the Brønsted line defined by the stronger acids; it does not show the positive deviation of 10–50-fold that is required for diffusion-controlled proton transfer.[5] (4) The rate constants for catalysis by chloroacetic acid (p$K = 2.65$) were found to exhibit no decrease with increasing viscosity in solutions containing up to 60% glycerol. (5) The calculated Brønsted curve for a preassociation mechanism,[7,9] shown as the solid line in Figure 1, provides a satisfactory fit to the experimental data.

Cordes and co-workers[10] observed intersecting Brønsted lines for catalysis of the methoxyaminolysis of *p*-nitrophenyl acetate and suggested that the break is caused by bifunctional, acid–base catalysis by carboxylic acids. The data in Figure 1 show that bifunctional catalysis by the stronger acids does not cause a rate enhancement compared with monofunctional acids, but does provide an explanation for the greater catalytic effectiveness of weaker bifunctional catalysts. The fact that these rate constants are larger than those for simple monofunctional catalysts in the region in which monofunctional catalysis is limited largely by the k_p step requires either concerted proton transfers or additional stabilization by hydrogen bonding with the bifunctional catalysts.

The solvent isotope effects for monofunctional catalysts show a sharp maximum at p$K = 6.8$ (Figure 2), close to the calculated pK of 6.5 for T$^+$. Similar maxima have been observed for catalysis of nitramide decomposition[11] and for catalysis of methoxyamine addition to *p*-methoxybenzaldehyde by a trapping mechanism.[12] This isotope effect maximum confirms the existence of a kinetically significant proton transfer step in the preassociation mechanism when the ΔpK between the proton donor and acceptor is small.

The isotope effect maximum cannot be explained by the change in rate-determining step from k_1' to k_p to k_b (eq 1). The calculated isotope effects for this explanation[9] are shown as the dashed line in Figure 2 and are inconsistent with the observed isotope effects; in particular, the observed isotope effects fall off with increasing acid strength at much higher pK than the calculated line. Variation of the estimated maximum isotope effect and other parameters does not improve the agree-

ment. The decrease in the isotope effect with acid catalysts of p$K = 7$–4, for which the proton-transfer step is largely rate determining, requires a decrease in the isotope effect of the k_p step itself with increasing acid strength. The shape of the observed curve is attributed to a maximum in the isotope effect for the k_p step and to a decrease in the observed isotope effect as the k_b step becomes rate determining with weak acid catalysts.[13] The maximum may reflect asymmetric transition states for proton transfer,[15] tunneling,[16] or both in the proton-transfer step, k_p.

References and Notes

(1) Publication No. 1210 from the Graduate Department of Biochemistry, Brandeis University. Supported by grants from the National Science Foundation (BG-31740) and the National Institutes of Health (GM20888 and 5-T01-GM00212 (the latter to M.M.C.)).
(2) A. C. Satterthwait and W. P. Jencks, *J. Am. Chem. Soc.*, **96**, 7018, 7031 (1974).
(3) W. P. Jencks, *Acc. Chem. Res.*, **9**, 425 (1976).
(4) This type of mechanism has been called a "spectator" mechanism by Kershner and Schowen (*J. Am. Chem. Soc.*, **93**, 2014 (1971)) when the catalyst does not accelerate the rate-determining step.
(5) M. Eigen, *Angew. Chem., Int. Ed. Engl.*, **3**, 1 (1964).
(6) J. P. Fox and W. P. Jencks, *J. Am. Chem. Soc.*, **96**, 1436 (1974).
(7) H. F. Gilbert and W. P. Jencks, *J. Am. Chem. Soc.*, **99**, 7931 (1977).
(8) J. M. Sayer and W. P. Jencks, *J. Am. Chem. Soc.*, **95**, 5637 (1973).
(9) The theoretical curves[7,8] were calculated from eq 12 and 14 of ref 7, with p$K_{T^+} = 6.5$, $k_{HA} = 2 \times 10^{-4} M^{-2} s^{-1}$, $k_{-1} = 2 \times 10^{10} s^{-1}$, $\alpha = 0.16$, log $k_p = 11 + 0.5 \Delta pK$, log $k_{-p} = 11 - 0.5 \Delta pK$ ($\Delta pK = pK_{T^+} - pK_{HA}$), $k_b = k_{-a} = 10^{11} s^{-1}$. The dashed line in Figure 2 was calculated assuming a solvent deuterium isotope effect, k_{H_2O}/k_{D_2O}, of 5 for k_p and k_{-p} and 1.25 for k_{HA}, k_b, and k_{-a}.
(10) L. do Amaral, K. Koehler, D. Bartenbach, T. Pletcher, and E. H. Cordes, *J. Am. Chem. Soc.*, **89**, 3537 (1967).
(11) J. R. Jones, and T. G. Rumney, *J. Chem. Soc.*, *Chem. Commun.*, 995 (1975). (However, see footnote 4 of the accompanying paper[12].)
(12) N.-Å. Bergman, Y. Chiang, and A. J. Kresge, preceding paper in this issue.
(13) A theoretical curve that provides a satisfactory fit to the data, shown as the solid line in Figure 2, was calculated from the kinetic parameters for the preassociation mechanism[9] assuming a maximum isotope effect for k_p and k_{-p} of 11 for an acid of p$K = 7.25$ and an intrinsic barrier of $\Delta G_0^{\ddagger} = 0.6$ kcal mol^{-1} for the Marcus–Kresge treatment of isotope effects.[14] Although they are consistent with the data, these particular parameters are not unique.
(14) R. A. Marcus, *J. Phys. Chem.*, **72**, 891 (1968); A. J. Kresge, D. S. Sagatys, and H. L. Chen, *J. Am. Chem. Soc.*, **99**, 7228 (1977); R. More O'Ferrall, in "Proton Transfer Reactions", E. Caldin and V. Gold, Ed., Wiley, New York, N.Y., 1975, p 201.
(15) F. H. Westheimer, *Chem. Rev.*, **61**, 265 (1961).
(16) R. P. Bell, W. H. Sachs, and R. L. Tranter, *Trans. Faraday Soc.*, **67**, 1995 (1971); R. P. Bell, "The Proton in Chemistry", 2nd ed, Cornell University Press, Ithaca, N.Y., 1973, p 250.
(17) W. P. Jencks and M. Gilchrist, *J. Am. Chem. Soc.*, **90**, 2622 (1968).

Michael M. Cox, William P. Jencks*

Graduate Department of Biochemistry
Brandeis University, Waltham, Massachusetts 02154

Received May 2, 1978

### Fluorinated Rhodopsin Analogues from 10-Fluoro- and 14-Fluororetinal[1]

Sir:

The use of nuclear magnetic resonance spectroscopy in the vision field has largely been limited to the isolated chromophore. Both the ^{1}H NMR[2] and ^{13}C NMR[3] spectra of retinal isomers and their Schiff bases[4] have been analyzed in great detail. Application of the technique to probing structural information of the pigments directly, because of background noise, is expected to be difficult. However, with the use of a ^{13}C-enriched retinal, the ^{13}C spectrum of rhodopsin has been successfully recorded.[5] Fluorine-19 magnetic resonance spectroscopy will not have any background noise to contend with. However, it remains to be established that fluorine labeled pigment analogues do exist. To test this possibility we have synthesized isomers of 10-fluoro- and 14-fluororetinal (I and II). In this paper we describe the preparation and

Table I. ¹H NMR Signals of 10-Fluoro- (I) and 14-Fluororetinal (II) Isomers[a]

isomer	CH_3-1	CH_3-5	CH_3-9	CH_3-13	H_7	H_8	H_{10}	H_{11}	H_{12}	H_{14}	H_{15}	$J_{7,8}$	$J_{10,11}$	$J_{11,12}$	$J_{14,15}$
all-trans-1 (7E,9E,11E,13E)	1.06	1.76	1.99	2.35	6.28	6.68		6.85	6.69	6.05	10.10	16.1	25.1	15.5	8.0
7-cis-1 (7Z,9E,11E,13E)	1.06	1.51	1.83	2.31	6.08	6.56		6.73	6.65	6.02	10.09	13.0	25.6	16.0	7.6
9-cis-1 (7E,9Z,11E,13E)	1.04	1.73	1.99	2.34	6.24	6.34		6.88	6.62	6.04	10.10	15.6	27.3	15.5	7.9
11-cis-1 (7E,9E,11Z,13E)	1.06	1.75	1.93	2.34	6.25	6.60		6.31	6.12	5.91	10.04	16.1	30.6	12.5	7.8
13-cis-1 (7E,9E,11E,13Z)	1.06	1.76	1.99	2.16	6.28	6.67		6.70	7.58	5.87	10.23	16.1	27.5	15.7	7.8
7,9-di-cis-1 (7Z,9Z,11E,13E)	1.09	1.52	1.86	2.36	6.12	6.35		6.82	6.62	6.05	10.10	12.0	27.5	15.6	7.6
9,13-di-cis-1 (7E,9Z,11E,13Z)	1.05	1.74	2.01	2.16	6.26	6.32		6.78	7.54	5.86	10.23	16.0	26.2	15.3	8.0
7,9,13-tri-cis-1 (7Z,9Z,11E,13Z)	1.08	1.51	1.85	2.15	6.08	6.33		6.74	7.51	5.86	10.22	13.0	25.0	15.6	7.8
all-trans-11 (7E,9E,11E,13E)	1.04	1.72	2.04	2.27	6.26	6.14	6.23	7.02	6.79		9.75	16.2	11.5	15.2	12.8
7-cis-11 (7Z,9E,11E,13E)	1.06	1.54	1.93	2.26	5.96	6.11	6.30	6.96	6.75		9.85	12.0	b	b	12.4
9-cis-11 (7E,9Z,11E,13E)	1.06	1.75	2.03	2.26	6.28	6.57	6.11	7.09	6.73		9.74	16.0	11.0	15.0	12.3
11-cis-11 (7E,9E,11Z,13E)	1.04	1.72	2.01	2.38	6.28	6.13	6.2[c]	6.71	6.4[c]		9.75	15.9	11.8	11.8	11.4
13-cis-11 (7E,9E,11E,13Z)	1.02	1.69	1.99	2.08	6.21	6.07	6.11	6.94	7.28		9.76	16.1	11.0	15.0	10.6
9,13-di-cis-11 (7E,9Z,11E,13Z)	1.02	1.70	1.98	2.05	6.22	6.53	6.06	7.0[c]	7.1[c]		9.74	15.6	b	b	10.8
11,13-di-cis-11 (7E,9E,11Z,13Z)	1.00	1.68	1.97	2.05	6.20	6.07	6.17	6.72	6.08		9.46	16.0	11.7	11.7	17.8

[a] Varian XL-100; 5% dioxane-d_8 in CCl_4 (by volume). [b] Chemical shift too close to allow accurate measurement. [c] Assignment may be reversed.

I

II
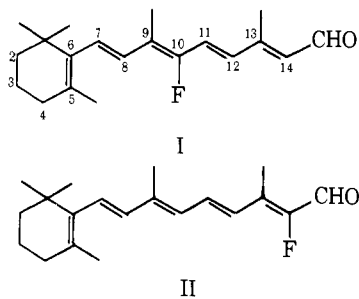
characterization of these isomers and properties of pigment analogues.

The preparation of several fluorinated vitamin A derivatives in the form of mixtures of the 13-cis and all-trans isomers of the acetates was first reported by Machleidt.[6] The reagents that he used in introducing a fluorine atom onto the polyene chain were the C_2 and C_5 phosphonates (III and IV). The reaction sequences that he followed were variations of the stan-

$(EtO)_2PCHCO_2R$, F — III

$(EtO)_2P$—...Y , CO_2R — IVa, Y = F; b, Y = H

Va, Y = H; b, Y = F

VI
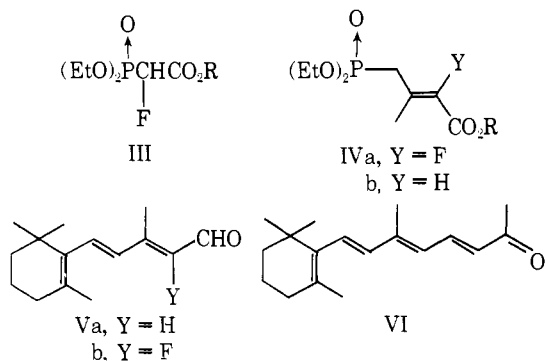
dard C_{15} + C_5 route (IV + V) in vitamin A synthesis.[7] We first adopted his method to prepare the 7-trans isomers of retinal. At the same time we showed the C_{18} + C_2 route[7] (VI + III) as an equally useful approach. Furthermore, starting with a mixture of the two 7-cis isomers of Va[8] and the 7,9-di-cis isomer of Vb, we obtained several of the 7-cis isomers of I and II.

Following these routes we prepared and isolated six geometric isomers (all-trans, 9-cis, 13-cis, 7,9-di-cis, 9,13-di-cis, and 7,9,13-tri-cis) of I and five (all-trans, 7-cis, 9-cis, 13-cis, and 9,13-di-cis) of II. Additionally, by direct irradiation of the trans isomers in acetonitrile,[9] we obtained several more hindered isomers of I (7-cis and 11-cis) and II (11-cis and 11,13-di-cis).[10] All these isomers were isolated by preparative high pressure liquid chromatography.[11]

Characterization of the geometry of all these isomers largely rest on the ¹H NMR data. The key chemical shift and coupling constant data are listed in Table I.[12] In analyzing the data, we found that many of the generalizations observed in the parent retinal system[2,8] are also applicable to these fluorinated analogues. Since these points are important in identifying the geometry of the polyene chain, they are briefly summarized below.

The magnitude of the vinyl coupling constants is an obvious indication of the geometry about the 7,8 and 11,12 double bonds. Additionally, the chemical shifts of CH_3-5 and H-12 signals are also indicative of the geometry around these two bonds: the CH_3-5 and H-12 signals for, respectively, the 7-cis and 11-cis isomers appear characteristically at a higher field (0.2 and >0.5 ppm) than those of the corresponding trans. The 9-cis geometry in II is indicated by low-field H-8 signals (0.4 ppm) due to steric depolarization[2c] and the 13-cis geometry by the upfield shift (0.2 ppm) of the CH_3-13 signals and the downfield shift (0.1 ppm) of H-15.[13]

Table II. Absorption Maxima of Isomers of 10-Fluoro- and 14-Fluororetinal and the Corresponding Pigment Analogues

	10-F, nm		14-F, nm	
isomer	retinal[a]	pigment[b]	retinal[a]	pigment[b]
all-trans	360	none	379	none
7-cis	347	484	369	none
9-cis	358	486	372	511
11-cis	340	502, 500[c]	370	527
13-cis	359	none	375	none
7,9-di-cis	347	464		
9,13-di-cis	353	484	369	513

[a] In hexane. [b] With digitonin. From difference spectra obtained immediately after addition of NH_2OH followed by bleaching with light at ≥ 500 nm. [c] Purified by column chromatography on hydroxylapatite with Ammonyx LO.

The only possible ambiguous point is the geometry about the 9,10 bond in I. The chemical-shift data cannot be rationalized by the steric depolarization explanation alone. The assignments in Table I follow the geometry of the triene aldehyde Vb which is unambiguously indicated by the chemical shift of CH_3-9. We assumed that the subsequent reactions did not change the stereochemistry at this center. Based on previous stereoselective synthesis of 7,9-di-*cis*- and 7,9,13-tri-*cis*-retinal,[14] the latter assumption appears to be a safe one.

The UV absorption maxima of the isomers of I and II (Table II) generally parallel those of the parent retinal;[15] i.e., the all trans isomer absorbs at the longest wavelength and 11-cis is the most blue shifted with the remaining isomers absorbing in between.

We have conducted experiments testing possible pigment formation of most of these isomers. Cattle rod outer segment suspensions or solutions of opsin solubilized in digitonin[16] were incubated at ≤ 30 °C[17] with isomers of I and II. The reaction was followed by UV-vis absorption spectroscopy. Pigment formation involving the binding site of opsin is again judged by the commonly accepted criteria of appearance of a new absorption band in the visible region and that the associated pigment is stable in the presence of a large excess of hydroxyl amine.

The absorption spectra of the pigment analogues are shown in Figures 1 and 2. Other data are also listed in Table II. 10-Fluororetinal behaves very similarly to the parent retinal in that all isomers except all-trans and 13-cis form stable pigments, and the absorption maxima of 9-cis and 11-cis pigment analogues are very similar to those of isorhodopsin and rhodopsin.[15,16b,18] The fluorine atom, therefore, does not have a significant effect on pigment formation. Since it is not significantly larger than hydrogen, on steric grounds this result is not unexpected. The corresponding isomers from 14-fluororetinal also readily form pigments, quite interestingly, with λ_{max} more red shifted than rhodopsin. There are, however, some distinct differences. For example the 7-cis isomer failed to form a pigment, and the pigments from other isomers are somewhat unstable. Upon standing at room temperature with excess NH_2OH (170 mM), pigment absorption decreased in intensity, but at rates ($t_{1/2}$ = 3.4, 4.5, 11 h for, respectively, 9-cis, 11-cis, and 9,13-di-cis isomers, 23 °C, pH 7) too slow to be due to random Schiff bases formed outside the binding site. At this stage, the exact cause of the degradation process is not clear, but, since in the absence of hydroxylamine the 11-cis pigment appears to be indefinitely stable, the degradation process does not appear to be an intrinsic property of the pigments.

These preliminary results clearly show that stable fluorinated rhodopsin analogues can be formed, and, in spite of the presence of the highly electronegative fluorine atom, the properties of the pigment analogues do not appear to be sig-
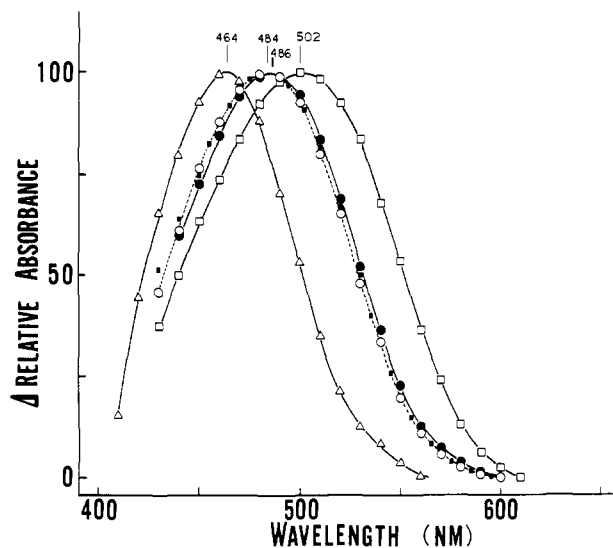
Figure 1. Normalized visible absorption spectra of visual pigments formed from 10-fluororetinal (I) (1% digitonin, room temperature): —□—, 11-cis; —●—, 9-cis; - -■- -, - -O- -, 7-cis and 9,13-di-cis; —△—, 7,9-di-cis.
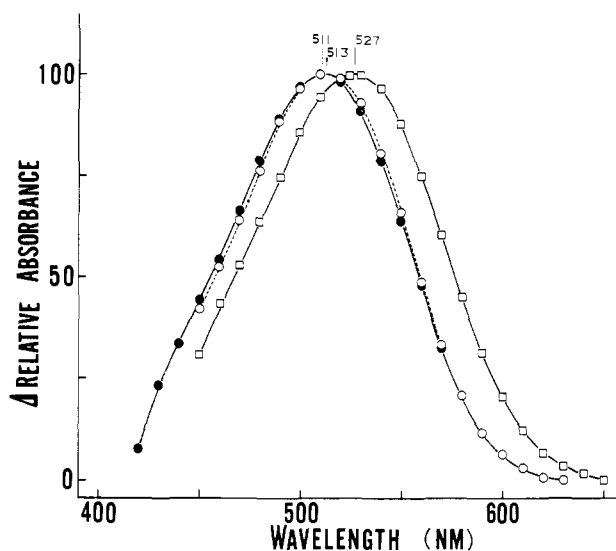
Figure 2. Normalized visible absorption spectra of visual pigments formed from 14-fluororetinal (II) (1% digitonin, room temperature): —□—, 11-cis; —●—, 9-cis; - -O- -, 9,13-di-cis.

nificantly different from those of rhodopsin and the corresponding isomers. Further detailed studies, including recording and analyses of the ^{19}F NMR spectra of the pigment analogues therefore appear well justified.

References and Notes

(1) New Geometric Isomers of Vitamin A and Carotenoids. 6. For paper 5, see ref 9c.
(2) (a) D. Patel, *Nature*, **221**, 825 (1969); (b) R. Rowan, III, A. Warshel, B. D. Sykes, and M. Karplus, *Biochemistry*, **13**, 970 (1974); (c) R. Rowan, III, and B. D. Sykes, *J. Am. Chem. Soc.*, **97**, 1023 (1975).
(3) (a) R. Rowan, III, and B. D. Sykes, *J. Am. Chem. Soc.*, **96**, 7000 (1974); (b) R. S. Becker, S. Berger, D. K. Dalling, D. M. Grant, and R. J. Pugmire, ibid., **96**, 7008 (1974); (c) Y. Inoue, A. Takahashi, T. Yokito, and R. Chujo, *J. Org. Magn. Reson.*, 487 (1974).
(4) (a) J. Shriver, E. W. Abrahamson, and G. D. Mateescu, *J. Am. Chem. Soc.*,

98, 2407 (1976); (b) G. M. Sharma and O. A. Roels, *J. Org. Chem.*, **20**, 3648 (1973).

(5) J. Shriver, G. Mateescu, R. Fager, D. Torchia, and E. W. Abrahamson, *Nature*, **270**, 271 (1977).

(6) H. Machleidt and R. Wessendorf, *Justus Liebigs Ann. Chem.*, **674**, 1 (1964); **679**, 20 (1964); **681**, 21 (1965).

(7) See H. Mayer and O. Isler in "Carotenoids", O. Isler, Ed., Birkhauser, Verlag, Basel, 1971, p 325.

(8) V. Ramamurthy, G. Tustin, C. C. Yau, and R. S. H. Liu, *Tetrahedron*, **31**, 193 (1975).

(9) (a) M. Denny and R. S. H. Liu, *J. Am. Chem. Soc.*, **99**, 4865 (1977); (b) K. Tsukida, A. Kodama, and M. Ito, *J. Chromatogr.*, **134**, 331 (1977); (c) R. S. H. Liu, A. E. Asato, and M. Denny, *J. Am. Chem. Soc.*, **99**, 8095 (1977).

(10) At least two more minor isomers of II were present, but these and the 11,13-di-cis isomer could result from degradation of the 11-cis isomer in a dark process. Isomers of I are thermally more stable.

(11) Altex ½ in. × 1 ft 5-μ Lichrosorb column, 10% ether in hexane for I and 5% ether in hexane for II.

(12) Assignments confirmed by computer simulated spectra. We thank Dr. T. Bopp for his instruction and the use of his program.

(13) A solvent mixture of 5% dioxane-d_8 in CCl_4 (by volume) was used for all ^1H NMR samples. The signal of isotopic impurity of dioxane (3.59 ppm) does not interfere with those of the retinal. Other NMR data, e.g., the four-bond H, F coupling constants, will be discussed in a future full paper.

(14) A. E. Asato and R. S. H. Liu, *J. Am. Chem. Soc.*, **97**, 4128 (1975).

(15) See, e.g., R. Hubbard, P. K. Brown, and D. Bownds, *Methods Enzymol.*, **18**, 615 (1971).

(16) (a) H. Matsumoto, K. Horluchi, and T. Yoshizawa, *Biochim. Biophys. Acta*, **501**, 257 (1978); (b) W. J. DeGrip, R. S. H. Liu, A. E. Asato, and V. Ramamurthy, *Nature*, **262**, 416 (1976).

(17) We found that incubation at high temperatures gave erratic results. For example, at 37 °C even *all-trans*-retinal (or some isomers produced at this temperature) gave pigments absorbing in the visible region.

(18) R. Crouch, V. Purvin, K. Nakanishi, and T. Ebrey, *Proc. Natl. Acad. Sci. U.S.A.*, **72**, 1538 (1975).

Alfred E. Asato, Hiroyuki Matsumoto
Marlene Denny, R. S. H. Liu*

Department of Chemistry, 2545 The Mall
University of Hawaii, Honolulu, Hawaii 96822
Received April 26, 1978

Interproton Distances for the β-Turn Residues of the Peptide Gramicidin S Determined from Nuclear Overhauser Effect Ratios

Sir:

We wish to report the determination of the distances between both Pro $C^\delta H$ protons and the Phe $C^\alpha H$ proton of the D-Phe-Pro sequence in gramicidin S, cyclo(D-Phe-Pro-Val-Orn-Leu)$_2$. They quantitatively confirm our earlier nuclear Overhauser effect (NOE) observations[1] and the conclusion that this sequence possesses a type II′ β-turn conformation. This measurement represents an accurate method of determining the angle ψ in peptides and specifically ψ (Phe) in gramicidin S. The calculated interproton distances approximate the sum of the Van der Waals radii of the two protons.

Both relaxation time and NOE measurements can in principle be used to determine interproton distances and dihedral angles in peptides.[1-7] Since the NOE's arise principally from dipolar coupling,[2,8,9] their determination by difference double resonance[1] or INDOR[1] promises significant advances in conformational analysis of complex peptides in solution.

The proton magnetic resonance spectra and difference double resonance spectrum of gramicidin S obtained by irradiating the Pro $C^{\delta 2}H$ are shown in Figure 1. The value of all six NOE's shown in Figure 2 were obtained by comparing the areas of the observed NOE's in double resonance difference spectra with the area of the $C^\alpha H$ region of the normal spectrum. Cancellation of nondipolar coupled resonances are better than 0.5% in all cases.

Even though the extreme narrowing condition is not met ($\tau_c \sim 10^{-9}$ s here[5]), the ratios of NOE's and the interproton distances are still related[8] as shown in eq 1–3 where, for example, $NOE_{\delta 1}(\delta 2)$ is the fractional intensity change in the resonance
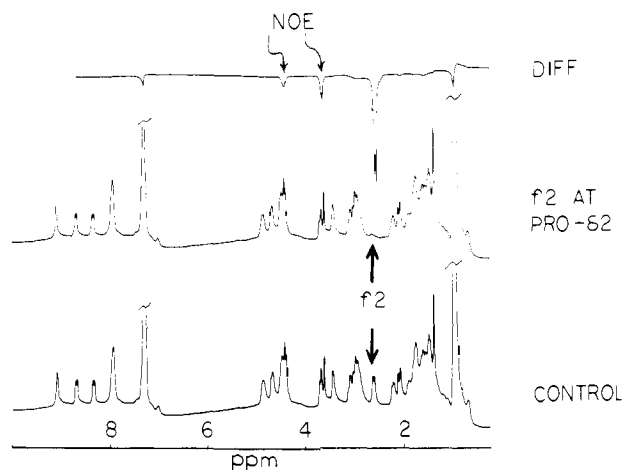

Figure 1. Three ^1H NMR spectra are shown: a "control" spectrum with the decoupling frequency set off resonance, a spectrum obtained with the decoupler frequency set to irradiate the Pro $C^{\delta 2}H$, and the difference obtained by subtracting the former from the latter spectrum. The two NOE's discussed in the text are indicated by arrows.
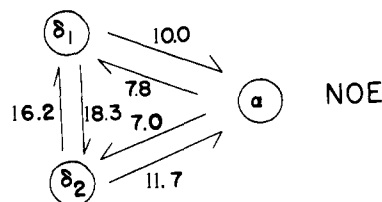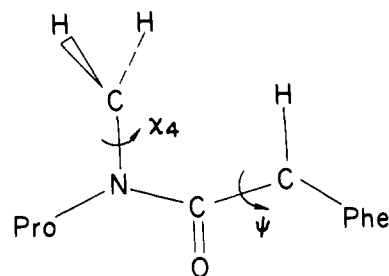

Figure 2. The fragment of gramicidin S containing the Phe $^4C^\alpha H$ and the two Pro $C^\delta H$'s is shown. Also shown are the values of the six NOE's (the arrows point from the irradiated proton to the proton at which the stated percent decrease in intensity is observed).

from the Pro $C^{\delta 1}H$ when the Pro $C^{\delta 2}H$ is irradiated and $r_{\delta 1-\alpha}$ is the interproton distance between the Pro $C^{\delta 1}H$ and the Phe $C^\alpha H$.

$$\frac{r_{\delta 1-\alpha}}{r_{\delta 1-\delta 2}} = \left[\frac{NOE_{\delta 1}(\delta 2) + NOE_{\delta 1}(\alpha)NOE_\alpha(\delta 2)}{NOE_{\delta 1}(\alpha) + NOE_{\delta 1}(\delta 2)NOE_{\delta 2}(\alpha)}\right]^{1/6}$$
$$= 1.15 \quad (1)$$

$$\frac{r_{\delta 2-\alpha}}{r_{\delta 2-\delta 1}} = \left[\frac{NOE_{\delta 2}(\delta 1) + NOE_{\delta 2}(\alpha)NOE_\alpha(\delta 1)}{NOE_{\delta 2}(\alpha) + NOE_{\delta 2}(\delta 1)NOE_{\delta 1}(\alpha)}\right]^{1/6}$$
$$= 1.21 \quad (2)$$

$$\frac{r_{\alpha-\delta 1}}{r_{\alpha-\delta 2}} = \left[\frac{NOE_\alpha(\delta 2) + NOE_\alpha(\delta 1)NOE_{\delta 1}(\delta 2)}{NOE_\alpha(\delta 1) + NOE_\alpha(\delta 2)NOE_{\delta 2}(\delta 1)}\right]^{1/6}$$
$$= 1.04 \quad (3)$$

The internuclear distance between the two Pro $C^\delta H$'s can easily be obtained by using the C–H bond length of 1.1 Å and a H–C–H angle of 107°.[10] This value of 1.77 Å plus the ratios above $r_{\delta 1-\alpha} = 2.03$ and $r_{\delta 2-\alpha} = 2.14$ for the distances between each Pro $C^\delta H$ and the Phe $C^\alpha H$. This use of NOE ratios for determining interproton distances is well established[8] and ^{13}C relaxation studies[11] have demonstrated that all carbon atoms